New techniques for reconstructing and calibrating hadronic objects with ATLAS

Magda Diamantopoulou (Carleton University)
On behalf of the ATLAS collaboration

Boost2024, Genoa (Italy)
29 July 2024

Outline

- Jets are experimental signatures of quarks and gluons in high energy processes.
    - They are built: .
        - with anti-k_t algorithm of cone size R=0.4 or 1.0.
        - using constituents which combine information from charged particle tracks and calorimeter energy deposits:
            - PFlow: combines tracks and topo clusters
            - UFO: combines PFlow and Track Calo Cluster methods, which correct the topo-cluster spatial coordinates with matched track information at high p_T.
- Detector-level jets need to be **calibrated** to the truth level, in order to compensate for detector and reconstruction-based limitations.
- Developments in the **reconstruction** and **calibration** of hadronic objects and **missing transverse momentum** will be presented.
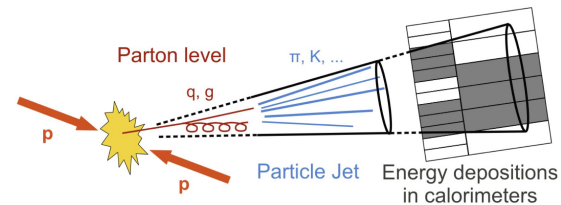
Jet production
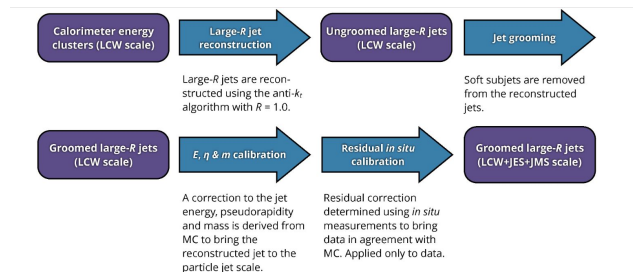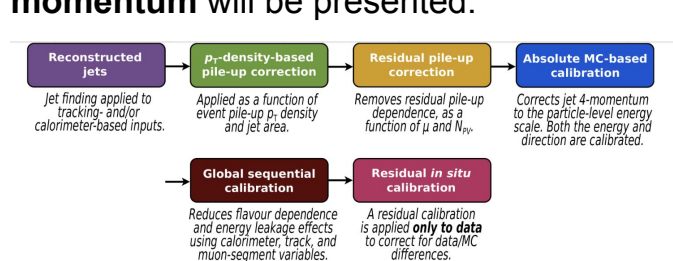
Calibration chain for small-R and large-R jets

2

The 'cell-time' cut

- Calorimeter topo clustering is based on the cell energy significance $|E|/\sigma_E$
  - Seeds are the cells passing $|E|/\sigma_E > 4$. Then there is an iterative collection of neighbouring cells.

- Cell-time information has been added recently to the topological clustering algorithm as additional discriminator:
  - Cut at $|t| < 12.5$ ns for any cell that has $|E| > 4\sigma$ and restrict the time cut to those cells with $E < 20\sigma$
    - suppresses out-of-time jets while retaining in-time signals: about -**60%** at $p_T = 20$ GeV
    - Avoids rejecting phase space potentially sensitive to Long-Lived particles signals with higher significance.
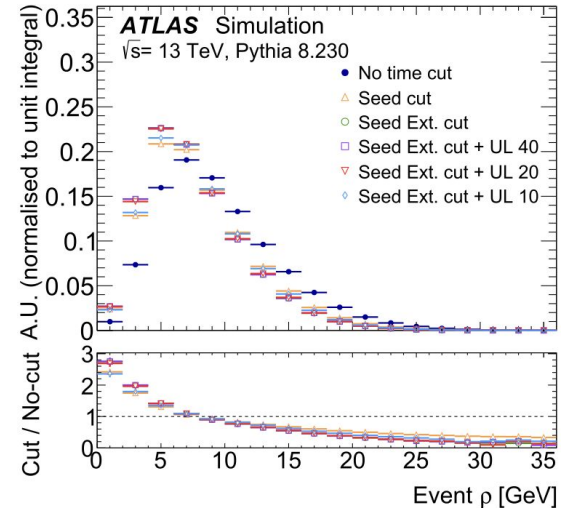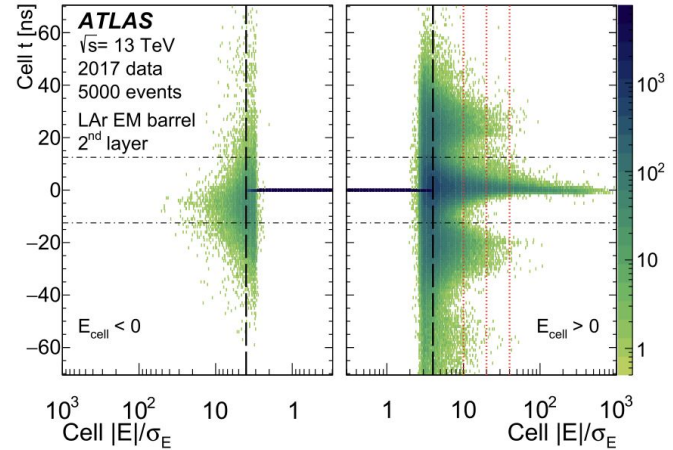
Topocluster calibration using Machine Learning techniques

- The current version of the topocluster calibration is the Local hadronic Cell Weighting (LCW) which aims to correct for hadronic non-compensation, and energy losses due to out of cluster and out of calorimeter deposits
  - This is done using cluster moments and lookup tables to have an associated weight according to the probability of having a hadronic or electromagnetic cluster.

- New approach: Application of **Machine Learning** to topocluster calibration.
  - Using a regression technique, with similar input features as the ones used in LCW and also mu and NPV to include pileup information.
  - Tested already on the correction of hadronic non-compensation.
  - Architectures being used:
    - Deep and Bayesian Neural Networks (DNN, BNN)
   - DNN performs better than BNN.
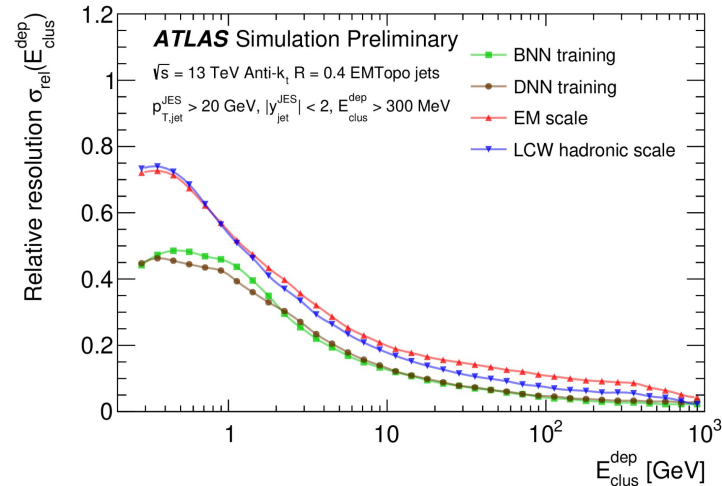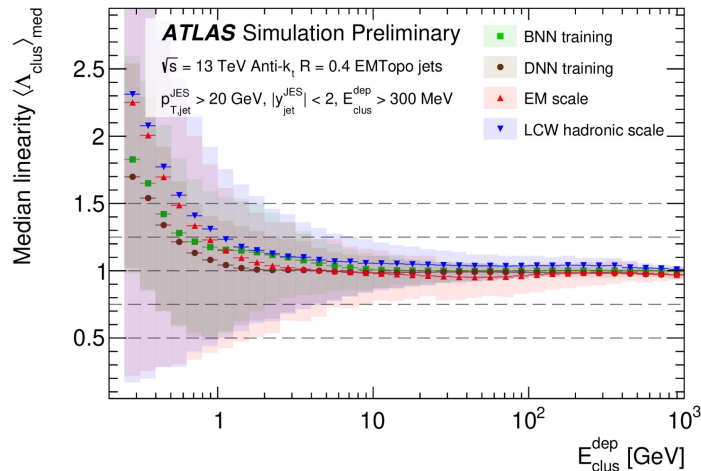
Global calibration and Global Neural Network Calibration

- The first stage of the calibration uses simulation to derive corrections to the Jet Energy Scale (JES) in order to reduce the impact of pile-up and detector effects.
  - After the MC JES calibration, **the Global Sequential Calibration (GSC)** is applied to jets, accounting for differences between the calorimeter response to different types of jets.
  - The GSC uses many kinematic uncorrelated observables in addition to p_T and the JES remains unchanged.

- **GNNC** is an alternative procedure, that uses DNN with jet observables (that can also be correlated) and is allowed to change the JES. The additional observables are:
  - 12 more layer energy fractions, number of clusters with 90% of energy and pileup observables
- GNNC **improves** the resolution by 15-25% and the JES closure at low p_T

5
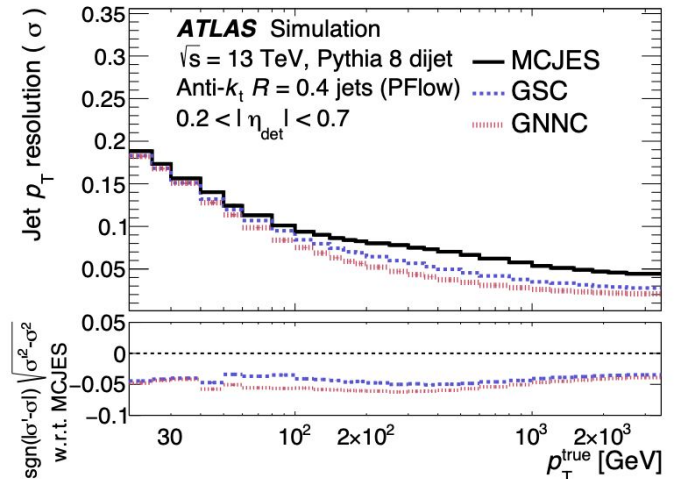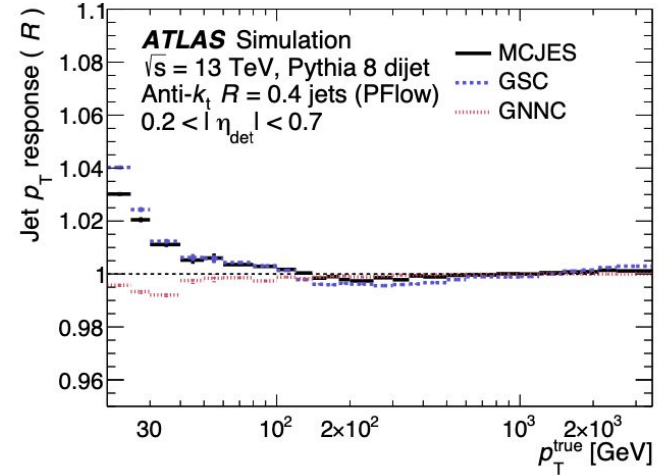
Jet Energy Scale for bottom quarks

- Dedicated b-JES in-situ calibration is aiming:
  - to improve the resolution of b-JES by taking into account the different nature of b-jet
  - To calculate the uncertainties of the b-JES:
    - It should reduce systematics but constituent based taggers have more generator dependance.
    - It might be the same for regression techniques - work on-going.

- New technique: Based on the GN2 and GN2X flavour-tagging models.
  - two different regression models were trained:
    - one for PFlow small-R jets and another one for UFO large-R jets
  - Both models utilise the **transformer network architecture.** Jet and track inputs are concatenated and the combined jet-track sequence vectors are fed into a per-track initialiser network.

- Performance of small-R jets shows **18-31%** better p_T resolution.
- Performance of large-R jets shows improvement on the mass and p_T resolution of **25-35%**
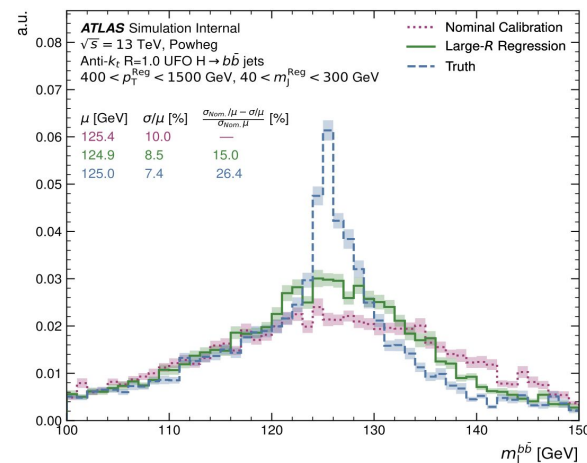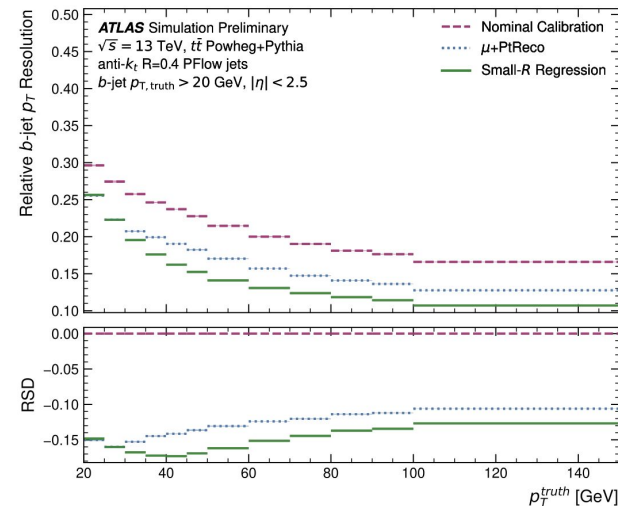
E/p method: In situ JES derived from single particle measurements

- JES is derived by shifting and smearing each particle in the jet by the measured calorimeter response and uncertainties.
  - Traditionally measured in minimum bias collisions using isolated tracks and having limited kinematic reach up to 20 GeV.
- New single particle measurement with W→ $\tau\nu$ events opens up new possibility for precise measurement of JES.
  - Extends the kinematic region up to 300 GeV.

- Improvement achieved with combination of standard p_T balance and single particle response based JES (especially in high p_T region)

- The single-particle response measurements are generic, and can be used for any type of jet :
  - q/g jets, jets with different R, boosted jets
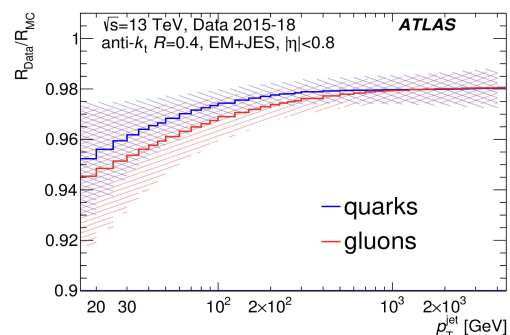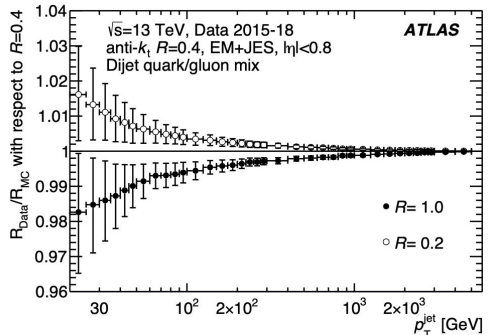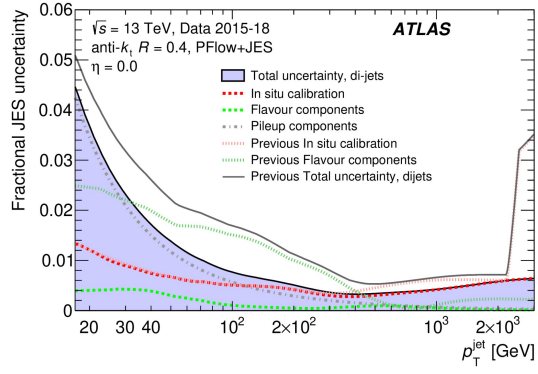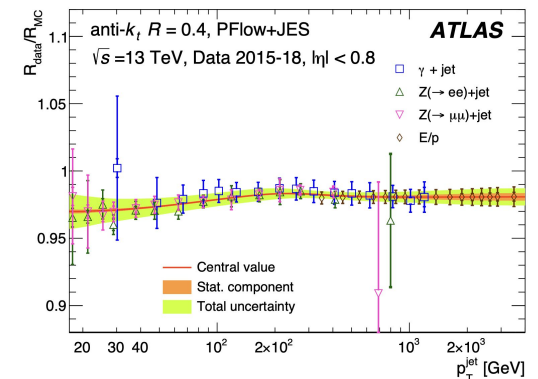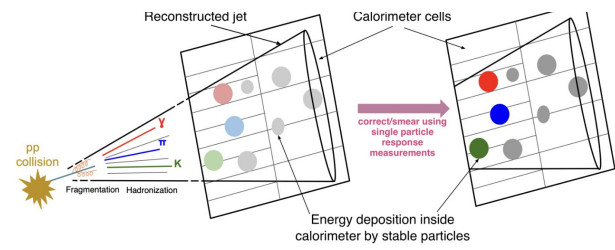
Using pile-up for physics [1]
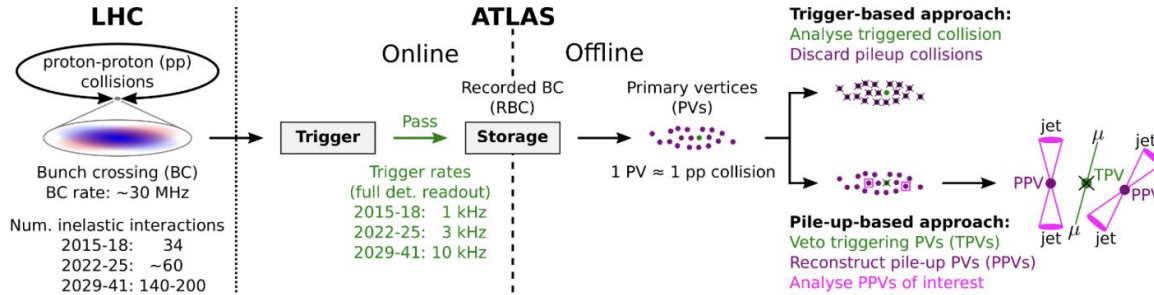
- New reconstruction strategy to increase the statistics for hadronic processes at low energy
- The Triggering Primary Vertex can be removed and jets from other vertices are used to reconstruct **pile-up.**
  - Use only jets from the same collision.
  - Use only well understood jets within the tracker coverage
  - Remove out-of-time jets
- With this approach we have more data compared to the single-triggers with p_T < 65 GeV.
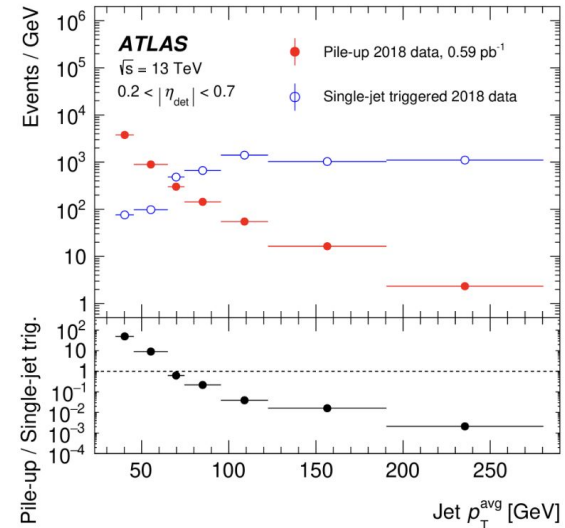
Using pile-up for physics [2]

- Dijet asymmetry defined with randomly selected probe and reference jets using jets in region 0.2 < |η| < 0.7

$$\mathcal{A} \equiv \frac{p_T^{probe} - p_T^{ref}}{p_T^{avg}}$$

- Such a measurement is an excellent way of demonstrating the validity of the pile-up dataset.
- The statistical power of the pile-up dataset against the single-jet triggered data directly, shows that pileup sample has reduced statistical uncertainties at low p_T
- The pile-up dataset is **unbiased,** since the results are compatible with the ones from the combined single-jet triggered measurement (dijet balance and random cones).

ATLAS
√s = 13 TeV
$0.2 < |\eta_{det}| < 0.7$

- Pile-up-based dijet JER, 2017 data, 0.47 pb^{-1}
- Single-jet triggered dijet JER, 2017 data, EPJC 81 (2021) 689
- ATLAS in situ JER measurement, 2017 data, EPJC 81 (2021) 689

ATLAS
√s = 13 TeV
$0.2 < |\eta_{det}| < 0.7$

- Pile-up-based dijet JER, 2017+2018 data, 1.06 pb^{-1}
- NSC-fit to the pile-up-based dijet JER
- ATLAS in situ JER measurement, 2017 data, EPJC 81 (2021) 689

arXiv:2407.10819
and poster from V.Cepaitis!

9
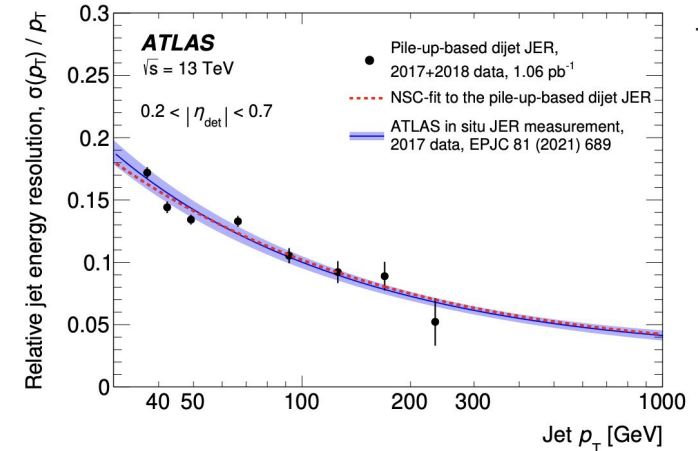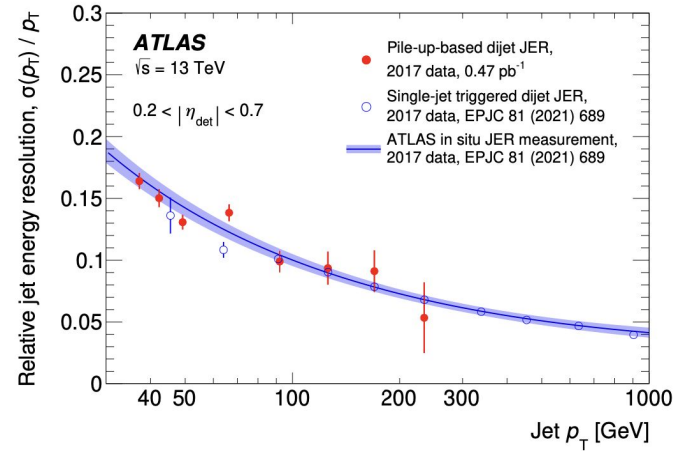
Calibration of large-R jets using Deep Neural Network

- Simultaneous calibration of **energy** and **mass** of UFO Constituent Subtraction-Soft Killer (CSSK) large-R jets using one DNN.

- Jet energy response of the DNN calibration is closer to unity than the standard calibration.

- Jet energy resolution is significantly improved with the DNN calibration.

- Jet mass response of boosted massive jets (W/Z, Higgs boson and top-quark decay) shows the improvements of the DNN calibration compared with the standard one

arXiv:2311.08885
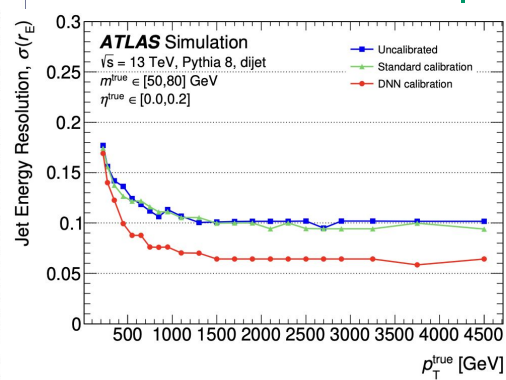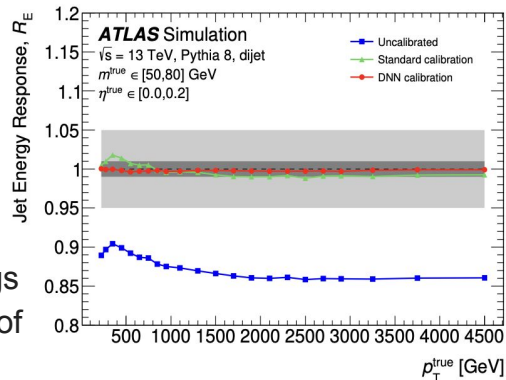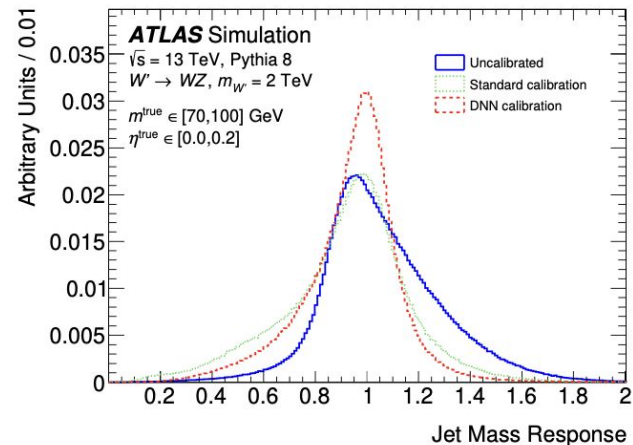
Missing Transverse Momentum [1]

- Use of momentum conservation in *x-y* plane to estimate the p_T of undetected particles
  - Important for searches of beyond-SM particles like dark matter .

$$\boldsymbol{p}_T^{miss} = - \left| \underbrace{\underbrace{\sum_{\substack{selected \\ electrons}} \boldsymbol{p}_T^e + \sum_{\substack{accepted \\ photons}} \boldsymbol{p}_T^\gamma + \sum_{\substack{accepted \\ \tau-leptons}} \boldsymbol{p}_T^\tau + \sum_{\substack{selected \\ \mu}} \boldsymbol{p}_T^\mu + \sum_{\substack{accepted \\ jets}} \boldsymbol{p}_T^{jet}}_{hard\ term} + \underbrace{\sum_{\substack{unused \\ tracks}} \boldsymbol{p}_T^{track}}_{soft\ term}} \right|$$

- In Z → μμ events no p_T^{miss} is expected:
  - Overall good data/MC comparisons
  - Dominant systematic in p_{Thard} from JES.
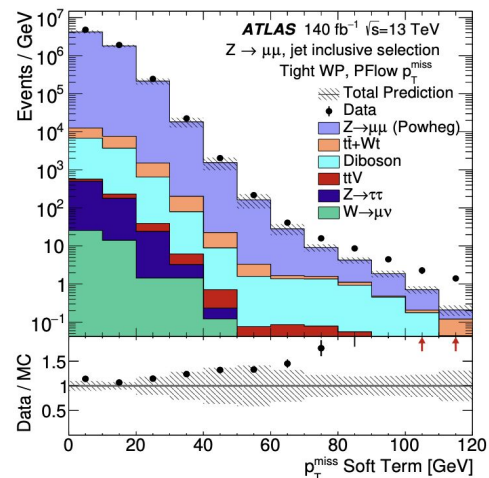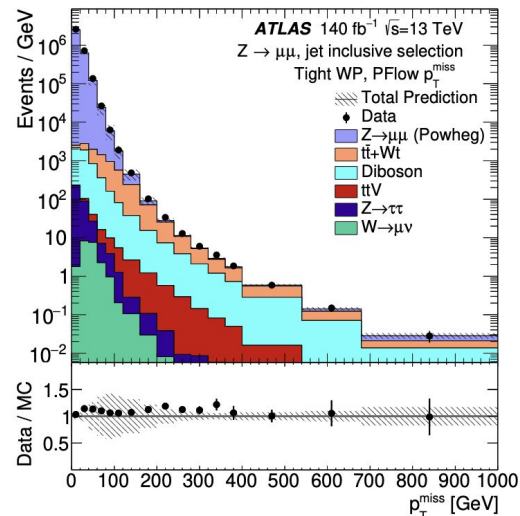
Missing Transverse Momentum [2]

- The **soft term's uncertainty** is calculated by considering the projection of the soft term onto the hard term
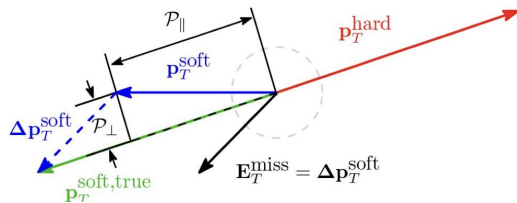
- p_T^{miss} **significance** is an important quantity which helps to discriminate signal from background, in the context of searches for new physics

$$\mathcal{S}(p_T^{miss}) = \frac{p_T^{miss}}{\sqrt{\sigma_L^2 \left(1 - \rho_{LT}^2\right)}}$$

- σ_L defines the longitudinal resolution to p_T^{miss} and ρ_{LT} defines the correlations between transverse and longitudinal resolution relative to p_T^{miss}

- The low values are dominated by events with an expected truth p_T^{miss} of zero, which have some fake p_T^{miss}

- The high valued tails are more dominated by events from other processes that have a high energy neutrino produced.
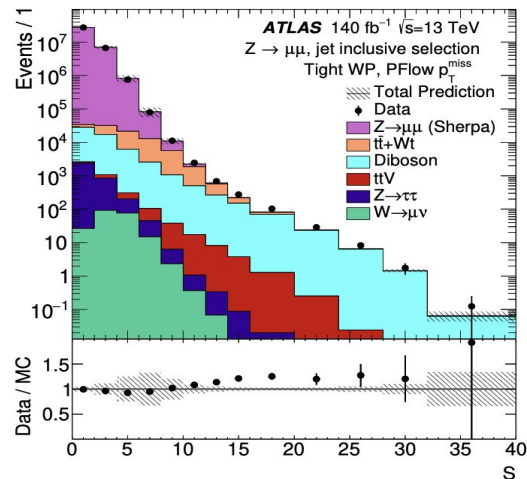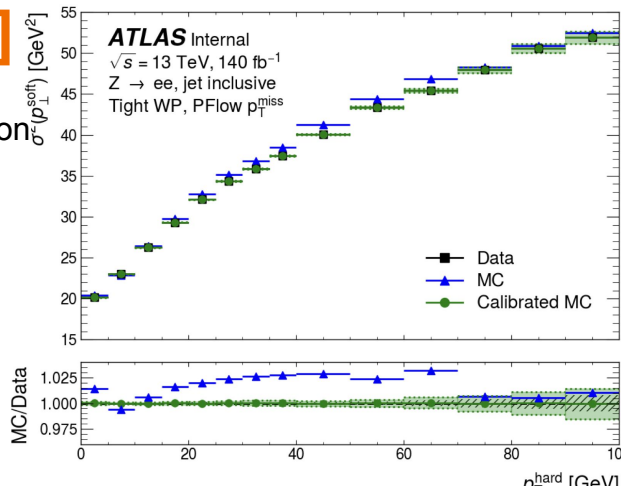
Conclusions

- Significant improvements on reconstruction and calibration of hadronic objects in ATLAS:
  - Pileup mitigation by introducing the cell-time cut in the topoclustering algorithm.
  - Reconstruction of the missing transverse momentum and its significance, with important impact on dark matter searches
  - New techniques to extend the energy/mass regions and the accuracy of the standard jet calibration methods.
    - New ML-based techniques have been explored.
  - Novel approach to use pile-up collisions to increase the statistics for low energy hadronic processes.
- Summary of all public plots for BOOST, prepared by the ATLAS Outreach Group: https://atlas.cern/Updates/News/Summary-BOOST-2024,

- Stay tuned for new ideas and further improvements!

Thank you!

Back up

Missing Projection fraction (MPF) method
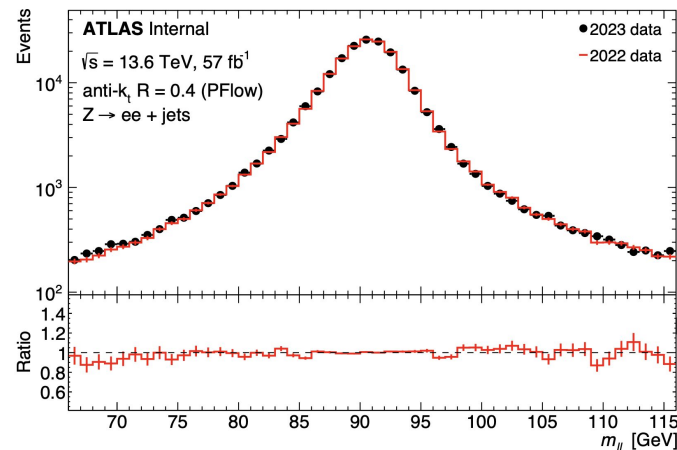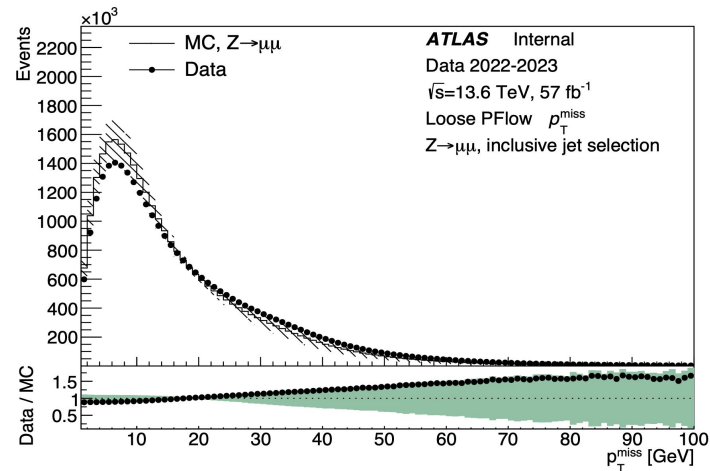
- The in situ calibration aims to correct the jet response between simulation and data. It consists of several steps
    - Z/γ +jet
    - Eta-intercalibration
    - Multi-jet balanced methods.

- The MPF method is used the use of the hadronic system recoiling against the Z/γ and It allows to improve uncertainties and kinematic reach at low pT.

$$\mathcal{R}_{MPF} = \left\langle 1 + \frac{\hat{n}_{ref} \cdot \vec{E}_T^{\,miss}}{p_T^{ref}} \right\rangle$$
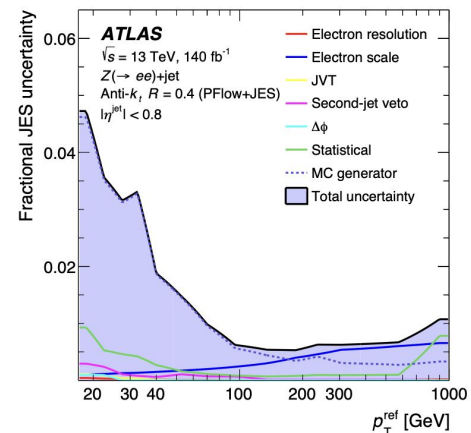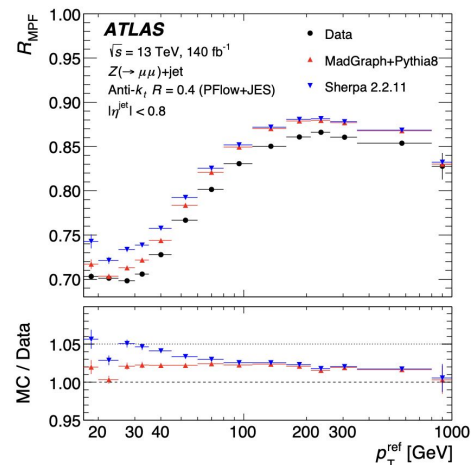
b- Jet Energy Scale

- b-JES is motivated by the improvement of **the (b-)jet energy resolution** in the context of H → b̄b analyses.

- Jets were tested against well measured γ, using the Direct Balance method.

- b-jets correction was found to differ from the one for inclusive jets.
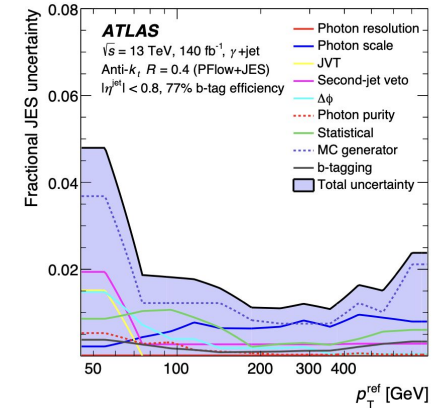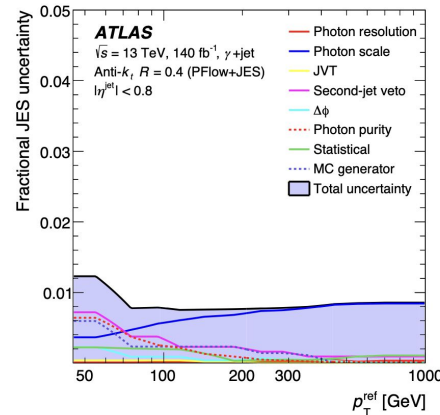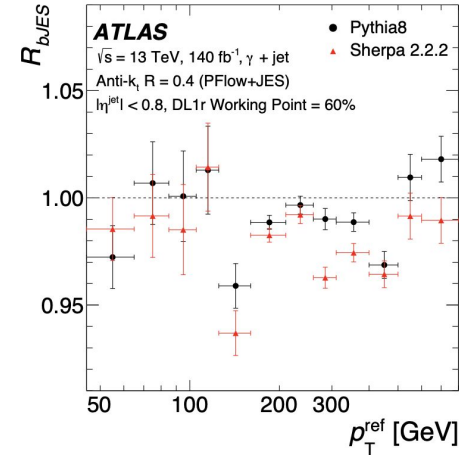
b-JES

Jet Feature	Description
p_T	Transverse momentum
η	Signed pseudorapidity
m ‡	Jet mass

Track & Charged UFO Feature	Description
q/p	Track charge divided by reconstructed momentum
$d\eta$	Pseudorapidity of track relative to the jet η
$d\phi$	Azimuthal angle of the track, relative to the jet ϕ
d_0	Transverse IP: Closest distance from track to beam-line in the transverse plane
$z_0 \sin\theta$	Longitudinal IP: Closest distance from track to PV in the longitudinal plane.
$\sigma(q/p)$	Uncertainty on q/p
$\sigma(\theta)$	Uncertainty on track polar angle θ
$\sigma(\phi)$	Uncertainty on track azimuthal angle ϕ
$s(d_0)$	Significance of transverse IP
$s(z_0 \sin\theta)$	Significance of longitudinal IP times the sin of the polar angle
nPixHits	Number of pixel hits
nSCTHits	Number of SCT hits
nIBLHits	Number of IBL hits
nBLHits	Number of B-layer hits
nIBLShared	Number of shared IBL hits
nIBLSplit	Number of split IBL hits
nPixShared	Number of shared pixel hits
nPixSplit	Number of split pixel hits
nSCTShared	Number of shared SCT hits
LeptonID †	Information on if the track was used in lepton reconstruction

Charged & Neutral UFO Feature	Description
p_T^{Flow} ‡	Transverse momentum of charged flow constituent
E_{Flow} ‡	Energy of charged flow constituent
$d\eta_{Flow}$ ‡	Pseudorapidity of track relative to the large-R jet η
$d\phi_{Flow}$ ‡	Azimuthal angle of the track, relative to the large-R jet ϕ
dr_{Flow} ‡	Angular distance of the track from the large-R jet direction

b-JES

| Soft Muon Input	Description
p_T	Transverse momentum
η	Signed pseudorapidity
ϕ	Azimuthal angle
dR	Angular distance of the soft muon from the small-R jet axis
q/p	Muon charge divided by the reconstructed momentum
Momentum Balance Significance	Ratio of the difference in momentum measured by the ID and MS to the uncertainty on the energy loss measured by the calorimeters
Scattering Neighbour Significance	Sum of the significances of the angular difference $\Delta\phi$ between pairs of adjacent hits along the track, multiplied by the particle charge
p_T^{rel}	Orthogonal projection of the muon p_T onto the jet axis
d_0	Transverse IP: Closest distance from track to beam-line in the transverse plane
z_0	Longitudinal IP: Closest distance from track to PV in the longitudinal plane
$\sigma(d_0)$	Uncertainty on measurement of transverse IP
$\sigma(z_0)$	Uncertainty on measurement of longitudinal IP
$d_0/\sigma(d_0)$	Significance of transverse IP
$z_0/\sigma(z_0)$	Significance of longitudinal IP

Soft Electron Input	Description
p_T^r	Relative p_T of the electron with respect to the jet
dR	Angular separation between electron and jet axis
p_T^{iso}	Isolation variable
$|\eta|$	Absolute value of pseudorapidity
$s(d_0)$	Transverse IP: Closest distance from track to beam-line in the transverse plane
$z(d_0)$	Longitudinal IP: Closest distance from track to PV in the longitudinal plane
$s(d_0/\sigma_{d_0})$	Significance of the transverse IP
$\Delta\phi^{res}$	$\Delta\phi$ The azimuthal angle difference $\Delta\phi$ between the cluster position in the middle layer and the track.
E/p	Ratio of the cluster energy to the track momentum
R_{had}	Ratio of E_T in the hadronic calorimeter to E_T of the EM cluster
R_{had1}	Ratio of transverse energy E_T in the first layer of the hadronic calorimeter to E_T of the EM cluster
E_{ratio}	Ratio of the energy difference between the largest and second largest energy deposits in the cluster over the sum of these energies
$w_{\eta 2}$	Lateral shower width
R_{eta}	Ratio of the energy in 3×7 cells over the energy in 7×7 cells centered at the electron cluster position
f_1	Ratio of the energy in the strip layer to the total energy in the EM accordion calorimeter
f_3	Ratio of the energy in the back layer to the total energy in the EM accordion calorimeter
p_{HF}	probability of being from heavy flavour decay

Topocluster calibration

The choice of features given to the network to learn $\mathcal{R}_{\text{clus}}^{\text{EM}}$ is driven by their potential sensitivity to electromagnetic and hadronic signal characteristics in the calorimeters,

A deposited energy – in a complex way represented by the topo-cluster signal $E_{\text{clus}}^{\text{EM}}$ itself;

B detector geometry – the signal characteristics of the various calorimeter subsystems in ATLAS contributing to the topo-cluster, like the level of non-compensation and the absorption power (leakage), as well as the energy sharing around the respective inactive transition regions between them;

C shower development – the differences between electromagnetic and hadronic showers in terms of starting point, size and signal compactness;

D intrinsic shower fluctuations – the variations in the shower development of hadronic showers;

E signal strength and relevance – signal significance measured by signal-over-noise;

F collision environment – effects of event topology/nearby signals and pile-up on the topo-cluster signal.

Pile-up
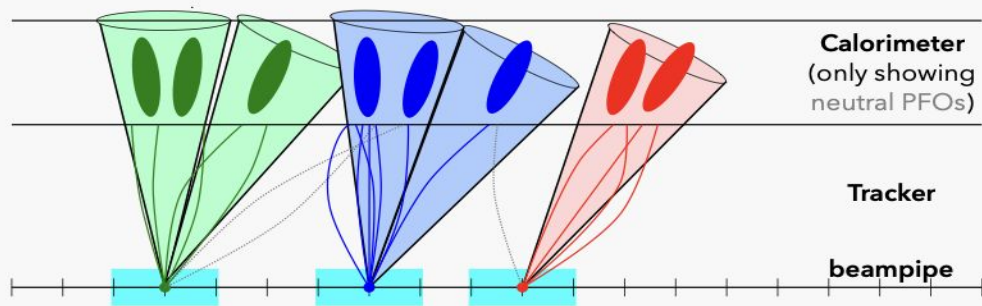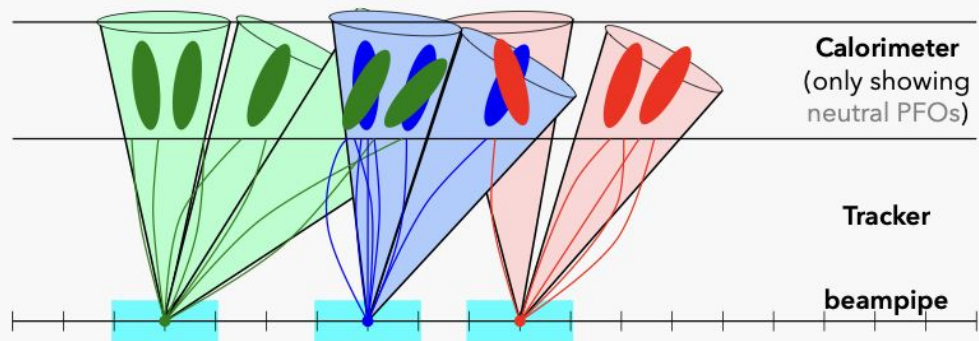
GSC

The six stages of the GSC, in the order of application, are

- f_{charged}: the fraction of the jet p_{T} carried by charged particles, as measured using ghost-associated tracks with $p_{\text{T}} > 500$ MeV, $|\eta^{\text{det}}| < 2.5$,

- f_{Tile0}: the fraction of jet energy (E_{frac}) measured in the first layer of the hadronic tile calorimeter, $|\eta^{\text{det}}| < 1.8$,

- f_{LAr3}: the E_{frac} measured in the third layer of the electromagnetic LAr calorimeter, $|\eta^{\text{det}}| < 3.5$,

- N_{track}: the number of tracks with $p_{\text{T}} > 1$ GeV ghost-associated with the jet, $|\eta^{\text{det}}| < 2.5$,

- w_{track}: also known as track width, the average p_{T}-weighted transverse distance in the η-ϕ plane, between the jet axis and all tracks of $p_{\text{T}} > 1$ GeV ghost-associated with the jet, $|\eta^{\text{det}}| < 2.5$,

- N_{segments}: the number of muon track segments ghost-associated with the jet, $|\eta^{\text{det}}| < 2.8$.

GNNC

Calorimeter	$f_{\text{LAr0-3*}}$	The E_{frac} measured in the 0th-3rd layer of the EM LAr calorimeter
	$f_{\text{Tile0*-2}}$	The E_{frac} measured in the 0th-2nd layer of the hadronic tile calorimeter
	$f_{\text{HEC,0-3}}$	The E_{frac} measured in the 0th-3rd layer of the hadronic end cap calorimeter
	$f_{\text{FCAL,0-2}}$	The E_{frac} measured in the 0th-2nd layer of the forward calorimeter
	$N_{90\%}$	The minimum number of clusters containing 90% of the jet energy
Jet kinematics	$p_{\text{T}}^{\text{JES}}$ *	The jet p_{T} after the MCJES calibration
	η^{det}	The detector η
Tracking	w_{track}*	The average p_{T}-weighted transverse distance in the η-ϕ plane between the jet axis and all tracks of $p_{\text{T}} > 1$ GeV ghost-associated with the jet
	N_{track}*	The number of tracks with $p_{\text{T}} > 1$ GeV ghost-associated with the jet
	f_{charged}*	The fraction of the jet p_{T} measured from ghost-associated tracks
Muon segments	N_{segments}*	The number of muon track segments ghost-associated with the jet
Pile-up	μ	The average number of interactions per bunch crossing
	N_{PV}	The number of reconstructed primary vertices

Table 1: List of variables used as input to the GNNC. Variables with a * correspond to those that are also used by the GSC.

23

Table 1: Overview of the input measurements and uncertainties used by the deconvolution method used for the calculation of the data-to-MC jet response correction.

Particle	p_T [GeV]	comment
hadrons	$p_T < 0.5$	5 % uncertainty
	$0.5 < p_T < 10$	isolated tracks in minimum bias collisions
	$10 < p_T < 300$	pions from τ-lepton decays in $W \to \tau\nu$ sample
	$p_T > 300$	MC out-of-range studies and using JES uncertainty constraint
e/γ	$5 < p_T < 200$	standard e/γ calibration from $Z \to e^+e^-$
		and 0.5% uncertainty for effects in jets
	$p_T > 200$	extrapolation based on electron calibration
	$p_T < 5$	additional 1% uncertainty from $\pi^0 \to \gamma\gamma$ mass peak constraint

Calibration of large-R jets using Deep Neural Network [2]

- Steps:
  - input processing: η annotation
    - compute additional features based on η to encode the proximity of the jet to the different regions of the detector to adapt to the complex response dependency on η
  - core : several dense layers which are common to both E and mass calibration
  - deep tail : early fork between E/m outputs
  - attention layers : helps the NN to learn which inputs are important for the mass calibration.
  - output: calibration factors for E and m